Materials Science and Engineering A xxx (2008) xxx–xxx

Contents lists available at ScienceDirect

Materials Science and Engineering A

journal homepage: www.elsevier.com/locate/msea

Three-dimensional numerical modelling of damage initiation in unidirectional fiber-reinforced composites with ductile matrix

Leon Mishnaevsky Jr.*, Povl Brøndsted

Risø National Laboratory for Sustainable Energy, Technical University of Denmark, AFM-228, P.O. Box 49, Frederiksborgvej 399, DK-4000 Roskilde, Denmark

ARTICLE INFO

Article history:
Received 25 December 2006
Received in revised form 6 September 2007
Accepted 24 September 2007
Available online xxx

Keywords:
Fiber-reinforced composites
Damage
Finite element analysis
Mesomechanics
Modelling

ABSTRACT

Three-dimensional finite element simulations of deformation and damage evolution in fiber-reinforced aluminium matrix composites are carried out. The fiber/matrix interface damage is modeled as a finite element weakening in the interphase layers. The fiber cracking is simulated as the damage evolution in the randomly placed damageable layers in the fibers, using the ABAQUS subroutine User Defined Field. The effect of matrix cracks and the interface strength on the fiber failure is investigated numerically.

1. Introduction

The purpose of this work is to analyze the damage evolution of fiber-reinforced metal matrix composites taking into account the microscale phase properties and the interaction between different damage modes.

The micromechanisms of damage in fiber-reinforced composites (FRC) can be described as follows [1]. If a fiber-reinforced composite with ductile matrix is subject to longitudinal tensile loading, the main part of the load is born by the fibers, and they tend to fail first. After weakest fibers fail, the load on remaining intact fibers increases. That may cause the failure of other, first of all, neighboring fibers. The cracks in the fibers cause higher stress concentration in the matrix, what can lead to the matrix cracking. However, if the fiber/matrix interface is weak, the crack will extend and grow along the interface. In the case of ceramic and other brittle matrix composites, the crack is formed initially in the matrix. If intact fibers are available behind the crack front and they are connecting the crack faces, the crack bridging mechanism is operative. In this case, the load is shared by the bridging fibers and crack tip, and the stress intensity factor on the crack tip is reduced. A higher amount of bringing fibers leads to the lower stress intensity factor on the crack tip, and the resistance to crack growth increases with increasing the crack length (R-curve behavior) [2,3]. The extension of a crack, bridged by intact fibers, leads to the debonding and pull out of fibers that increase the fracture toughness of the material.

In order to model the damage and failure of fiber-reinforced composites under mechanical loading, several approaches are used. Among them, the analytical, shear-lag based models (used often to analyze the load transfer and multiple cracking in composites) [4–9], the fiber bundle model (FBM) and its generalization [10,11], fracture mechanics-based models (which are applied quite often to the analysis of fiber bridging) [12–14] and, finally, micromechanical finite element models [[15–17], see also reviews in Refs. [1,18]] can be listed. One of the challenges of modelling damage and fracture in FRC is the necessity to take into account the interplay between the multiple fracturing in fibers, interface damage and debonding and the strongly nonlinear deformation behavior of the matrix.

In this work, we seek to apply the methods of the computational micromechanics to analyze the interaction between different damage mechanisms, and the effect of the phase and interface properties on the damage evolution in fiber-reinforced aluminium composites.

2. Finite element model generation and damage modelling

In order to automate the generation of three-dimensional (3D) micromechanical finite element models of composites, we developed a special program code "Meso3DFiber" [1]. The program, based on the approach to the automatic generation of 3D microstructural models of materials described in Refs. [1,19–21], is written in Compaq Visual Fortran. The program gen-

* Corresponding author.
E-mail address: leon.mishnaevsky@risoe.dk (L. Mishnaevsky Jr.).

0921-5093/$ – see front matter © 2008 Elsevier B.V. All rights reserved.
doi:10.1016/j.msea.2007.09.105

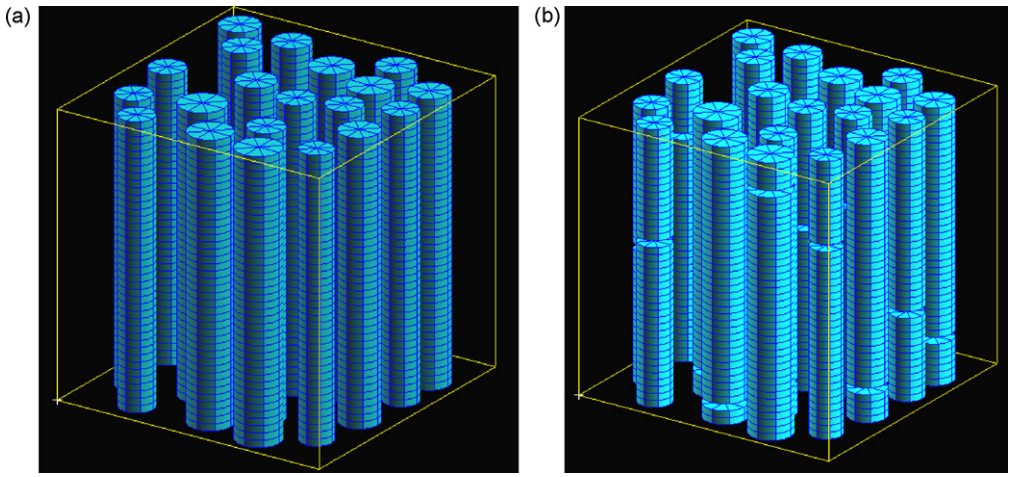

Fig. 1. Examples of the 3D unit cell models: a unit cell with 20 fibers with randomly varied radii (a) and the cell with removed damageable layers (b).

erates interactively a command file for the commercial software MSC/PATRAN. After the file is played with PATRAN, one obtains a 3D microstructural (unit cell) model of the composite with predefined parameters of its microstructure. The program allows to vary fiber sizes, the type of fiber arrangement (regular, random and clustered), volume content and amount of fibers. The finite element meshes were generated by sweeping the corresponding 2D meshes on the surface of the unit cell. The program is described in more details elsewhere [1,23].

The simulations were done with ABAQUS/Standard. The following properties of the phases were used in the simulations. The SiC fibers behaved as elastic isotropic damageable solids, with Young's modulus E_P = 485 GPa, and Poisson's ratio 0.165. The Al matrix was modeled as isotropic elasto-plastic damageable solid, with Young's modulus E_M = 73 GPa, and Poisson's ratio 0.345. The stress–strain curve for the Al matrix was taken from Refs. [19–21] in the form of the Ludwik hardening law: $\sigma_y = \sigma_{yn} + h\varepsilon_{pl}^n$, where σ_y is the actual flow stress, σ_{yn} = 205 MPa the initial yield stress, and ε_{pl} is the accumulated equivalent plastic strain, h and n are the hardening coefficient and the hardening exponent, h = 457 MPa, n = 0.20. The damage evolution in both fibers and in the interface layer was simulated, using the ABAQUS subroutine User Defined Field, described in Refs. [19–21,29].

According to Feih et al. [25], fiber failure is often triggered by fiber surface flaws, which are randomly located and are of random sizes. González and LLorca [17] proposed to simulate the fiber fracture in composites by placing damageable (cohesive/interface) elements along the fiber length and creating therefore potential fracture planes in the model. The random arrangement of the potential failure planes in this case reflects the statistical variability of the fiber properties. Following the idea by González and LLorca, we introduced damageable planes (layers) in several sections of fibers, and modeled the fiber cracking. The locations of the damageable layers in the fibers were determined using random number generator (uniform distribution). These layers have the same mechanical properties as the fibers (except that they are damageable). The damage evolution in these layers was modeled using the finite element weakening method [18,24]. The failure condition of fibers (in the damageable layers) was the maximum principal stress, 1500 MPa. Fig. 1 shows an example of a multifiber unit cell with 20 fibers of randomly varied radii, with and without the damageable layers.

In order to simulate the interface cracking of composites, the model of interface as a "third (interphase) material layer" was employed. The idea of the interphase layer model is based on the following reasoning. The surfaces of fibers are usually rather rough, and that influences both the interface debonding process and the frictional sliding. The interface regions in many composites contain interphases, which influence the debonding process as well [26,27]. Thus, the interface debonding does not occur as a two-dimensional opening of two contacting plane surfaces, but is rather a three-dimensional process in some layer between the homogeneous fiber and matrix materials. In order to take into account the non-planeliness (but rather fractal or three-dimensional nature) of the debonding surfaces and the debonding process, the interface damage and debonding are modeled as the damage evolution in a thin layer between two materials (fiber and matrix). This idea was also employed by Tursun et al. [28], who utilized the layer model to analyze damage processes in interfaces of Al/SiC particle reinforced composites. Fig. 2 shows an example of a multifiber unit cell with three fibers with interphase layer (yellow).

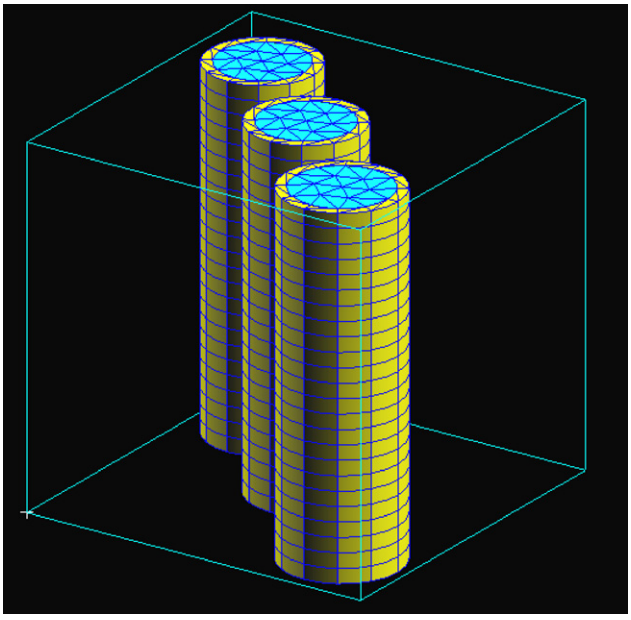

Fig. 2. Example: a unit cell with three fibers and interphase (yellow) layers. (For interpretation of the references to color in this figure legend, the reader is referred to the web version of the article.)

Please cite this article in press as: L. Mishnaevsky Jr., P. Brøndsted, Mater. Sci. Eng. A (2008), doi:10.1016/j.msea.2007.09.105

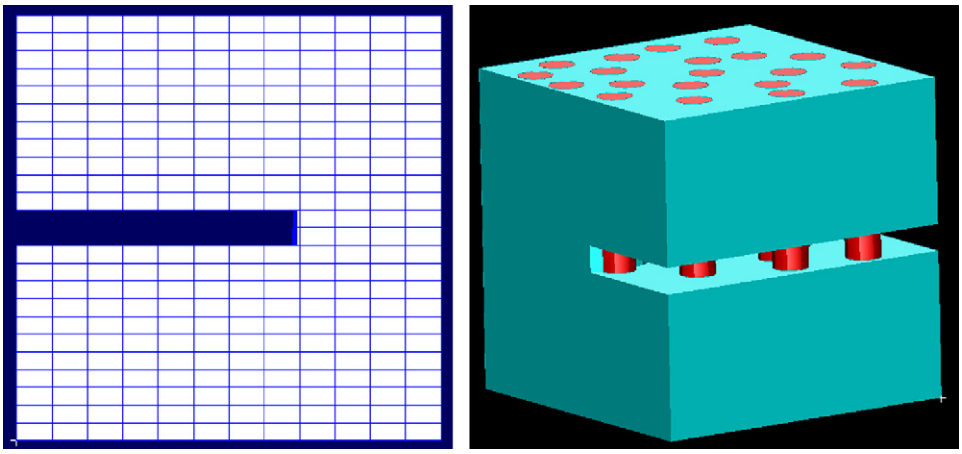

Fig. 3. Unit cell with a matrix crack and bridging fibers [1,23].

3. Numerical analysis of the effect of matrix cracks on fiber fracture

If a large crack or notch available in the matrix extends into the region with intact fibers, the matrix crack interacts with the fibers and influences their failures. In this section, we investigate the effect of cracks in the matrix on the fiber fracture. A number of three-dimensional multifiber unit cells with 20 fibers and volume content of fibers 25% have been generated automatically with the use of the program "Meso3DFiber" and the commercial code MSC/PATRAN. The fibers in the unit cells were placed randomly in *X*- and *Y*-directions. The cells were subject to a uniaxial tensile displacement loading, 0.1 of the cell size, along the axis of fibers (*Z*-axis). Further, three versions of the unit cells were generated, with introduced matrix cracks (notches). The cracks were oriented horizontally, normal to the fiber axis and loading vector. The lengths of the cracks were taken 16% ((1/6) of the cell size), 41% ((5/12) of the cell size), 66% ((8/12) of the cell size). The crack opening was taken 1/12 of the cell size (0.8 mm). Fig. 3 shows the general appearance of a cell with a matrix crack. At this stage of the work, the very strong fiber/matrix interface bonding was assumed, and only the effect of the matrix cracks on the fiber fracture was studied.

Fig. 4 shows the von Mises stress distribution in the fibers (in the unit cell with the matrix cracks) before and after the fiber cracking. The stresses are slightly lower in the regions of fibers adjacent to the matrix, which is attributed to the effect of the higher Poisson ratio in the matrix. After the fiber cracking, the stresses are rather low in the fiber regions close to the cracks, but increase with distance from the cracks (apparently, due to the load transfer via the shear stresses along the interface).

Fig. 5 shows the von Mises strain distribution in the matrix after the fiber failure. It is of interest to observe the shear bands, which tend to form in the matrix, connecting the regions of high stress concentration near the fiber cracks.

Figs. 6 and 7 give the stress–strain curves of the models and the damage (fraction of damaged elements in the damageable sections of the fibers) versus strain curves. One can see that the fiber cracking begins much earlier in the composites with the matrix cracks, than in non-cracked composites (apparently, due to the higher load in the bridging fibers, than in the fibers embedded in the matrix). The fiber failure leads to the much greater loss of stiffness in the composites with cracked matrix, than in non-cracked composites.

Now, let us consider the reverse effect: the effect of the fiber fractures on the damage initiation in the matrix. The composite (with cracks in fibers, modeled as layers with finite elements with

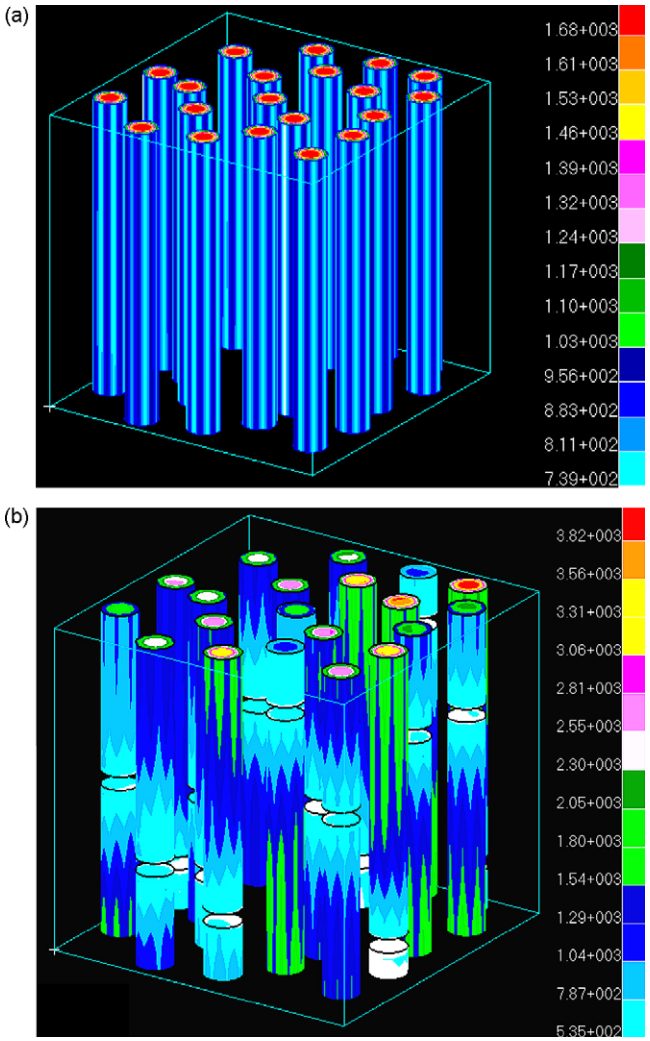

Fig. 4. von Mises stress distribution in the fibers before (a) and after (b) the fiber cracking. The cyclic distribution of the stresses along the circular boundary of fiber sections is due to the discrete (triangular finite elements) representation of the circular fiber sections.

Please cite this article in press as: L. Mishnaevsky Jr., P. Brøndsted, Mater. Sci. Eng. A (2008), doi:10.1016/j.msea.2007.09.105

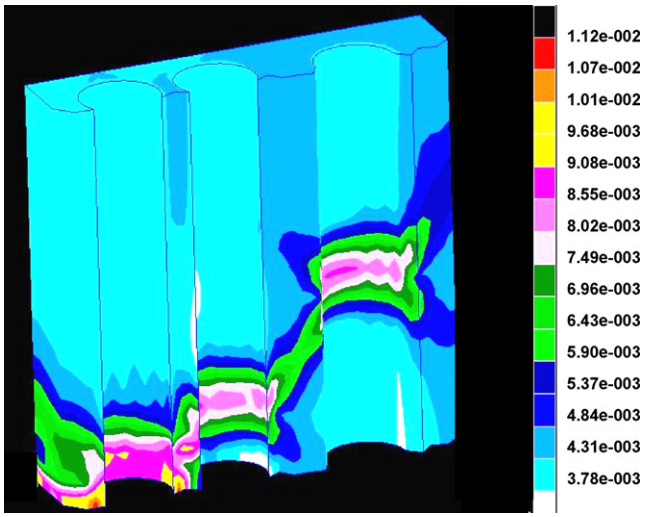

Fig. 5. von Mises strain distributions in the matrix after the fiber failure [1].

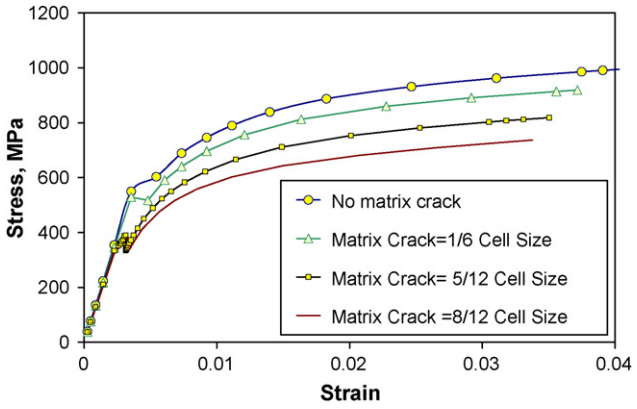

Fig. 6. Stress–strain curves for the unit cells with and without the matrix cracks.

reduced stiffness) with the initially undamaged matrix is loaded, until the matrix crackling begins. The void growth in aluminium matrix was modeled with the use of the Rice–Tracey damage criterion [30], implemented in the ABAQUS subroutine User Defined Field [21,22,29]. Fig. 8 shows the distribution of damaged areas in the matrix relative to the fibers (top view). It is of interest that the damage initiates in the matrix not between closely located fibers, but rather in random cites. However, at later stages of damage evolution (right picture) the cracks grow between closely located fibers.

4. Numerical simulations of interface damage and its interaction with matrix cracks and fiber fractures

Let us consider the interaction between all three damage modes in composites: matrix cracks, interface damage and fiber fracture. In order to model the interface damage, the model of interface as a "third layer" was used [26]. The interface layer was assumed to be a homogeneous isotropic material, with Young's modulus 273 MPa (i.e., the mean value of the Young's moduli of fiber and matrix) and Poisson's ratio of the matrix. The thickness of the layer was taken 0.2 mm. Following Tursun et al. [28], we chose the maximum principal stress criterion for the interface damage (therefore, assuming rather brittle interface). Two values of the critical stress were taken: 2000 MPa (i.e., strong, but still damageable interface) and 1000 MPa (weak interface). While the interface layer is considered as a homogeneous material in the first approximation, the model can be further improved if the graded material model is used to represent the interface layer, with properties to be determined from the inverse analysis [1].

Unit cells (with 15 fibers and 25% fiber volume content) were generated, and tested (with different strengths of interface layers). The unit cells without matrix cracks as well as with the cracks (notches) of 0.3 (short crack) and 0.58 of the cell size (long crack)

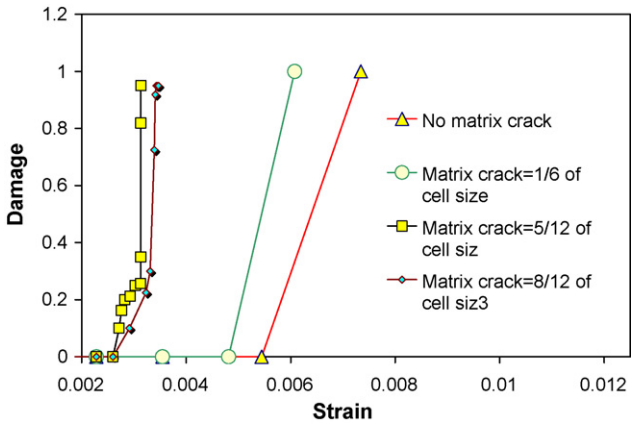

Fig. 7. Damage (fraction of damaged elements in the damageable sections of the fibers) versus strain curves for the unit cells with and without the matrix cracks [1].

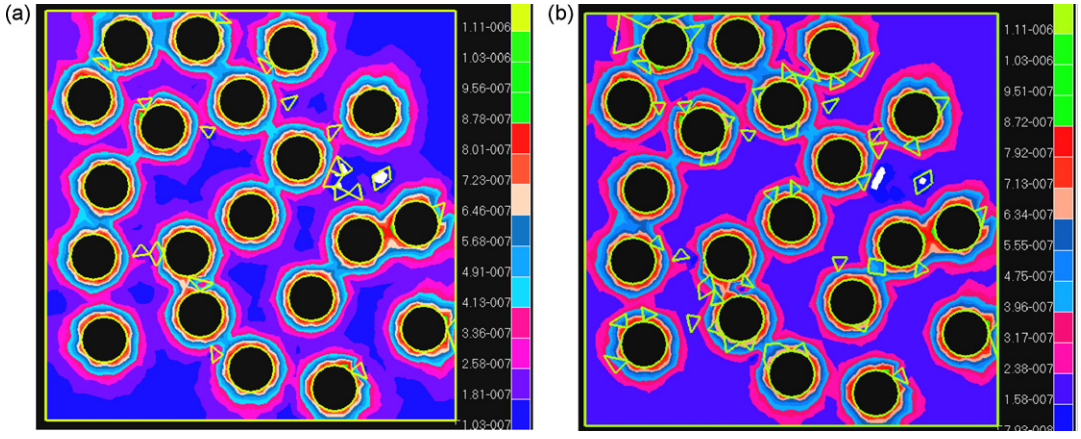

Fig. 8. Damage evolution (void growth) in the matrix triggered by the fiber fractures (top view).

Please cite this article in press as: L. Mishnaevsky Jr., P. Brøndsted, Mater. Sci. Eng. A (2008), doi:10.1016/j.msea.2007.09.105

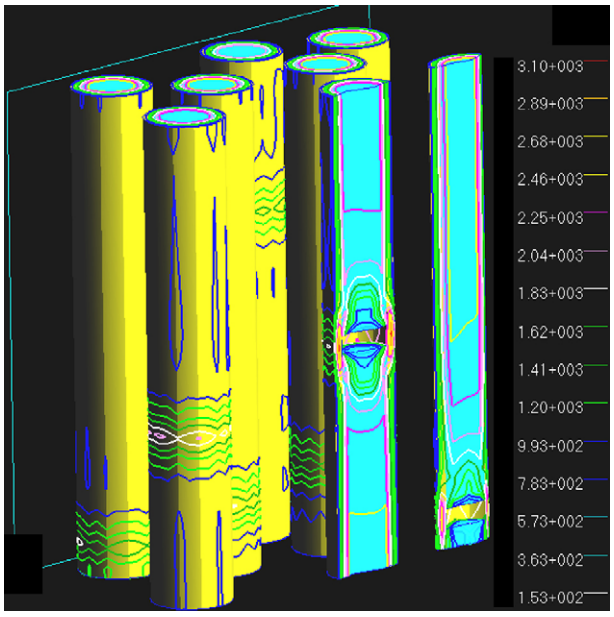

Fig. 9. von Mises stresses in the interface layer in the vicinity of the cracked fibers.

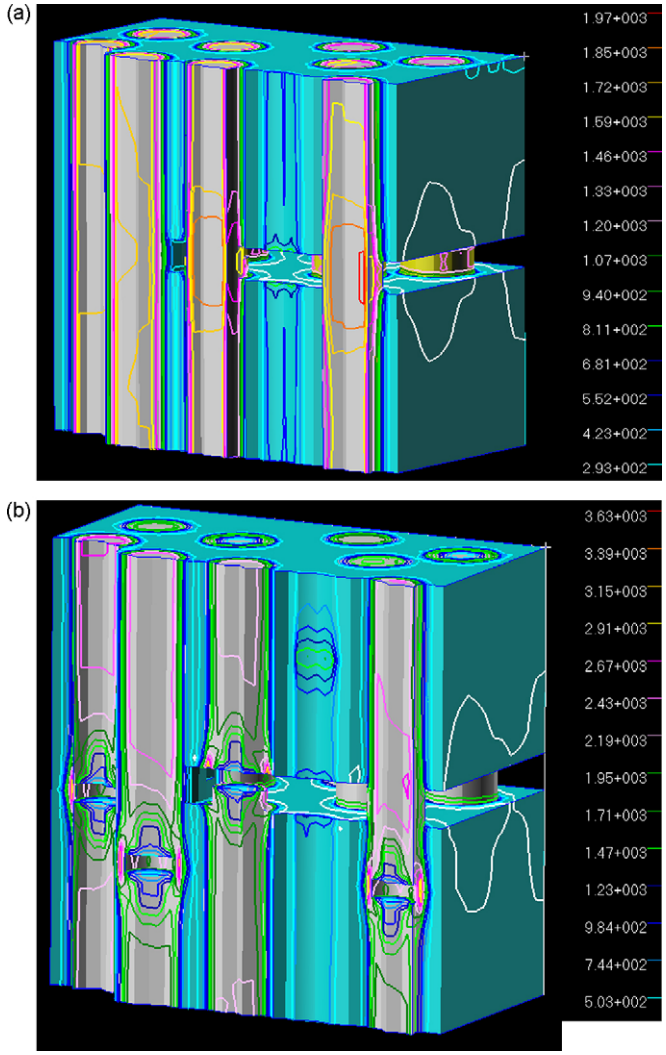

Fig. 10. von Mises stresses in the unit cell with the matrix crack and the interface layer before (a) and after (b) the fiber failure.

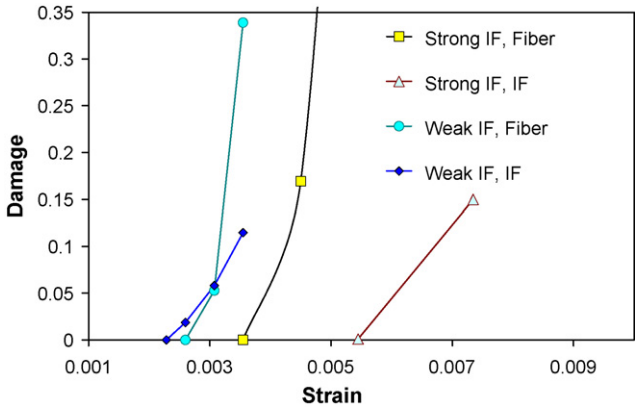

Fig. 11. Damage-strain curves for fibers and interface damage for the strong (failure stress 2000 MPa) and weak (failure stress 1000 MPa) interfaces [1]. The unit cell with the longer matrix crack (0.58 of the cell size) is considered.

were analyzed. The fiber arrangement in the cells with and without matrix cracks was the same.

Fig. 9 shows von Mises stress distribution in stresses in the interface layer in the vicinity of the cracked fibers. Fig. 10 shows von Mises stress distribution in the fibers and in the interface layer before and after the fiber cracking (the case of the longer matrix crack, and of the strong damageable interface). The section in the unit cell corresponds to 0.276 of the cell size. One can see that the fiber cracking leads to the high stress concentration at the interfaces of the composite in the vicinity of the fiber cracks.

It is seen that the fiber failed not in the sections along the matrix crack, but rather in the pre-defined damageable layers. This reflects the fact that we assumed that the fiber cracking is controlled first of all by the heterogeneities/weak sites in fibers, and only in the second place by the stress distribution in the material (see Section 2). A further improvement of this model could be assuming all the layers/planes along the fiber length to be damageable, with different failure conditions and probabilities.

Fig. 11 shows the damage (fraction of failed elements) in fibers and in the interface plotted versus the applied strain, for the case of strong and weak interfaces, and the cracked matrix (long crack). In the case of the strong interface, the interface damage growth starts at a somewhat higher strain than the fiber cracking, and begins in the vicinity of the fiber cracks. Apparently, the interface damage growth is triggered by the fiber cracking. In the case of the weaker interface, the interface damage is not triggered by the fiber cracking, but precedes the fiber cracking: while in the unit cells with the stronger interfaces the interface damage begins only after the fibers fail (at the strain 0.005), in the unit cells with weak interfaces the interface damage begins at the strain 0.003. Feih et al. [31] observed experimentally the formation of interface cracks before the fragmentation of fibers in the unidirectional composites with weak interface.

One should note that the results shown in Fig. 11 are relevant only for the initial stage of the interface crack formation. The interaction between a long interface and long matrix crack is beyond the limits of this study.

5. Conclusions

Computational simulations of the deformation and damage evolution in fiber-reinforced aluminium matrix composites are presented. New techniques of modelling of fiber fracturing and the interface damage are proposed and employed: the finite element

Please cite this article in press as: L. Mishnaevsky Jr., P. Brøndsted, Mater. Sci. Eng. A (2008), doi:10.1016/j.msea.2007.09.105

weakening in the layers (sections) of the fibers, randomly placed along the fiber length (for the modelling of fiber cracking), and the element weakening in the interphase layer between the fibers and matrix (for the modelling of the interface damage). Using these new methods and the developed techniques of the automatic generation of 3D microstructural models of composites, we investigated numerically the effect of the matrix cracks and the interface strength on the fiber failure.

Acknowledgement

The authors gratefully acknowledge the financial support of the Royal Danish Ministry of Foreign Affairs via the Danida project "Development of wind energy technologies in Nepal on the basis of natural materials" (Danida Ref. No. 104. DAN.8-913), and the European Community via "UpWind" project.

References

[1] L. Mishnaevsky Jr., Computational Mesomechanics of Composites, John Wiley and Sons, Chichester, 2007, 290.
[2] B.F. Sørensen, T.K. Jacobsen, Composites A 29 (1998) 1443–1451.
[3] B.F. Sørensen, T.K. Jacobsen, Plast. Rubber Compos. 29 (2000) 119–133.
[4] A.M. Sastry, S.L. Phoenix, Mater. Sci. Lett. 12 (1993) 596–599.
[5] C.M. Landis, I.J. Beyerlein, R.M. McMeeking, J. Mech. Phys. Solids 48 (2000) 621–648.
[6] I.J. Beyerlein, S.L. Phoenix, J. Mech. Phys. Solids 44 (1996) 1997–2039.
[7] I.J. Beyerlein, S.L. Phoenix, Eng. Fract. Mech. 57 (1997) 241–265.
[8] Z.H. Xia, W.A. Curtin, Compos. Sci. Technol. 61 (2001) 2247–2257.
[9] Z. Xia, W.A. Curtin, T. Okabe, Compos. Sci. Technol. 62 (2002) 1279–1288.
[10] F. Kun, S. Zapperi, H.J. Herrmann, Eur. Phys. J. B17 (2000) 269–279.
[11] F. Raischel, F. Kun, H.J. Herrmann, Phys. Rev. E 73 (2006) 066101–66112.
[12] D.B. Marshall, B.N. Cox, A.G. Evans, Acta Metall. 33 (1985) 2013–2021.
[13] L.N. McCartney, Proc. R. Soc. Lond. A 409 (1987) 329–350.
[14] W.S. Slaughter, Int. J. Solids Struct. 30 (1993) 385–398.
[15] L.E. Asp, L.A. Berglund, R. Talreja, Compos. Sci. Technol. 56 (1996) 657–665.
[16] N. Vejen, R. Pyrz, Compos. Part B: Eng. 33 (2002) 279–290.
[17] C. González, J. LLorca, Acta Mater. 54 (2006) 4171–4181.
[18] L. Mishnaevsky Jr., S. Schmauder, Appl. Mech. Rev. 54 (2001) 49–69.
[19] L. Mishnaevsky Jr., Acta Mater. 52 (2004) 4177–4188.
[20] L. Mishnaevsky Jr., Mater. Sci. Eng. A 407 (2005) 11–23.
[21] L. Mishnaevsky Jr., Compos. Sci. Technol. 66 (11–12) (2006) 1873–1887.
[22] L. Mishnaevsky Jr., Damage and Fracture of Heterogeneous Materials, Balkema, Rotterdam, 1998, 230 pp.
[23] L. Mishnaevsky Jr, P. Brøndsted, Micromechanisms of Damage Evolution in Glass Fiber Reinforced Polymer Composites: Numerical Study, in preparation.
[24] L. Mishnaevsky Jr., N. Lippmann, S. Schmauder, Int. J. Fract. 120 (2003) 581–600.
[25] S. Feih, A. Thraner, H. Lilholt, J. Mater. Sci. 40 (2005) 1615–1623.
[26] T.D. Downing, R. Kumar, W.M. Cross, L. Kjerengtroen, J.J. Kellar, J. Adhes. Sci. Technol. 14 (2000) 1801–1812.
[27] Y. Huang, J. Petermann, Polym. Bull. 36 (1996) 517–524.
[28] G. Tursun, U. Weber, E. Soppa, S. Schmauder, Comput. Mater. Sci. 37 (2006) 119–133.
[29] K. Derrien, D. Baptiste, D. Guedra-Degeorges, J. Foulquier, Int. J. Plast. 15 (1999) 667–685.
[30] J.R. Rice, D.M. Tracey, J. Mech. Phys. Solids 17 (1969) 201–217.
[31] S. Feih, K. Wonsyld, D. Minzari, P. Westermann, H. Lilholt, Testing Procedure for the Single Fiber Fragmentation Test. Risø-R-1483(EN), Risø National Laboratory, Roskilde, Denmark, 2004, p. 30.

Please cite this article in press as: L. Mishnaevsky Jr., P. Brøndsted, Mater. Sci. Eng. A (2008), doi:10.1016/j.msea.2007.09.105